# 15B.1 THE FAA TERMINAL CONVECTIVE WEATHER FORECAST PRODUCT: SCALE SEPARATION FILTER OPTIMIZATION* †

T.J. Cartwright, M.M. Wolfson, B.E. Forman, R.G. Hallowell, M.P. Moore, and K.E. Theriault
Massachusetts Institute of Technology
Lincoln Laboratory
Lexington, Massachusetts 02420-9185

## 1. INTRODUCTION

A large percentage of serious air traffic delay at major airports in the warm season is caused by convective weather. The FAA Convective Weather Product Development team (PDT) has developed a Terminal Convective Weather Forecast product (TCWF) that can account for short-term (out to 60 min) systematic growth and decay of thunderstorms.

The team began work three years ago by evaluating air traffic user needs and requirements. We found that users were willing to trade off forecast accuracy for longer lead times, especially for air traffic management plans that were easy to implement or that incurred low risk (Forman, *et al*., 1999). The PDT was able to develop an operationally useful forecast product that has been demonstrated in Dallas, TX since March, 1998 (Hallowell, *et al*., 1999). Further improvements have been made, and testing is now taking place at both Dallas and Orlando, FL.

This paper summarizes the basic algorithm methodology and presents quantitative results on optimization of the scale separation filter, which is an integral aspect of the forecast algorithm.

## 2. ALGORITHM METHODOLOGY

### 2.1 Envelope vs. Cell Motion

The Terminal Convective Weather Forecast product utilizes a method, dubbed the Growth and Decay Tracker[1] (Wolfson, *et al*., 1999), for tracking the storm envelope motion instead of the cell motion. By effectively tracking the storm scale forcing, the forecast product is able to account for the systematic growth and decay of organized convective systems. To extract this storm scale forcing, a filtering technique is applied to a 2-D base map of the Vertically Integrated Liquid water (VIL) made from NEXRAD wide-band data. These filtered images are tracked using the ITWS cross-correlation tracker with parameter settings optimized for this problem. The resultant vectors are used to advect the unfiltered weather images, producing an animated precipitation forecast in 10-minute intervals out to one hour.

Initially, a qualitative study was conducted to find the optimal filter size and aspect ratio for large scale convective features. A suite of 12 cases from Memphis, TN; Dallas, TX; and Orlando, FL was examined with filters of sizes (in km) of 5x15, 9x27, 15x45, 15x61, 21x105, and 37x181, having aspect ratios of 3:1, 4:1, and 5:1, respectively. The results revealed that a filter with an approximate size of 15x61 km (915 km$^2$) and an aspect ratio of 4:1 yielded the best approximated large-scale features in the test cases.

A line storm case from 1 June 1996 in Dallas was selected to illustrate the effect of elliptical filtering. In this case, the envelope motion and cell motion were quite different. Figure 1 shows the unfiltered "full-scale" image (VIL), the large-scale image (derived with the 15x61 km elliptical filter), and the small-scale image (derived by subtracting the result of a 15x15 km filter from the unfiltered image, thus selecting all scales less than 15x15 km). Within the large- and small-scale images the storm motion vector resulting from correlation tracking is shown. The large-scale signal is moving southeast at 34 knots, while the small-scale signal is moving northeast at 21 knots.

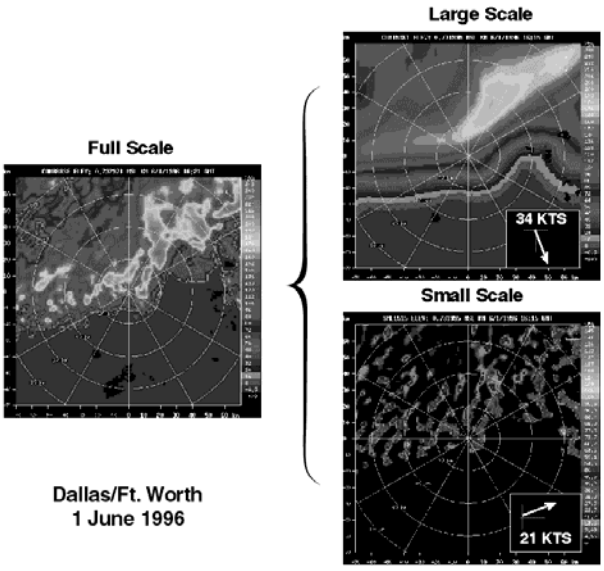


*Figure 1. The result of filtering full-scale image (left) with an elliptical filter to produce large-scale (top right) and small-scale (bottom right) images. The motion of the large-scale and small-scale components, found with a correlation tracker, are indicated (Wolfson,* et al*., 1999).*

* This work was sponsored by the Federal Aviation Administration. The views expressed are those of the authors and do not reflect the official policy or position of the U.S. Government.

† Opinions, interpretations, conclusions, and recommendations are those of the authors and are not necessarily endorsed by the United States Air Force.

Corresponding author information: Tina J. Cartwright, Massachusetts Institute of Technology, Lincoln Laboratory
e-mail: TINAC@LL.MIT.EDU phone: 781-981-0784

[1] Patent applied for by MIT.

### 2.2 Scoring Techniques

There are many different techniques for computing performance statistics. The most straightforward is a binary method, which is a simple pixel-by-pixel comparison of forecast and truth weather. However, this technique does not represent the value of the forecast to the users. When asked, users indicated that a one-hour forecast could be within 5 nm and still provide a valuable forecast. Therefore, a 5x5 pixel scoring kernel is used (giving a 400 $km^2$ verification area with 4 km pixels). A forecast is considered correct if a truth pixel is found within 10 km (5.4 nm) in any direction. Also, a Critical Success Index (CSI) statistic is used in lieu of the dual statistics Probability of Detection and Probability of False Alarm, both to reduce misunderstandings and simplify the display of forecast accuracy for users.

## 3. ALGORITHM APPLICATION

The performance of the TCWF depends on several variables. In Wolfson, *et al.* (1999), several important aspects of the TCWF were discussed. For example, the most robust choice for time interval between successive images to be correlated to produce the motion vectors was 12 min. This was selected as a compromise, since shorter times were good for air mass storms and longer times were better for line storms. (It was noted that this could be considered as a site-adaptable seasonal parameter.) Filtering was shown to be most valuable in cases in which a) there is some large-scale organization and b) systematic storm growth and decay cause propagation motion in a direction different than cell motion. This paper will present quantitative results on the size and shape of the filter used to extract the large-scale signal in the data, which is another important component of the TCWF.

### 3.1 Filter Optimization

Extracting the large-scale storm forcing is a critical component of the success of the TCWF. Past studies have shown that larger-scale features are most persistent in the atmosphere (e.g., Wilson, 1966). Other studies have examined different area averaging techniques to reduce the variance in forecasts. Bellon and Zawadzki (1994) conducted sensitivity tests on square filters to reduce rms errors in rainfall accumulation forecasts. They found the maximum correlation between the current image and the truth image 5-60 min in the future and compared the resultant correlation coefficients for different isotropic filters applied to the current image. An empirical relationship between the scale of the filtering and the forecast time period was derived. The effects of asymmetric weighting (based on storm shape) within a square filter were studied but were found to be negligible for one of their line storms.

This paper presents quantitative results on filter optimization studies maximizing the CSI scores. Each CSI score is the result of advecting an unfiltered VIL image according to track vectors derived by correlating two filtered images: the current image and one 12 min prior. The tracker parameter settings were discussed by Wolfson, *et al*. (1999). The advection scheme first advects the vector field 60 min in the future, fills holes using a Cressman filter, then turns every vector 180° and goes back 60 min to find the VIL value appropriate for that pixel (Hallowell, *et al*., 1999). By incorporating the precise methodology used in the forecast scheme as part of the filter size/shape optimization, we have tested the ability of the filter to select the most persistent scale matched to the 60-min forecast problem. Filtering of the current image, either prior to or after advection to produce the forecast image, is another source of variance reduction not explored in this study.

Filter optimization tests were conducted on 13 line storm cases from Dallas, TX; Orlando, FL; Boston, MA; and Memphis, TN. Dates can be seen in Table 1. All of these cases are line storms. Once filter optimization for this type of storm is complete, we will examine the effects of filter optimization on other types of convection.

*Table 1.*
*The CSI values for the optimal filter, the 3x17 filter, and no filter for the 13 line storm systems.*
*(The sizes of the optimal filters are shown in Figure 5.)*

| | | Optimal CSI | 3x17 | Unfiltered |
|---|---|---|---|---|
| DFW | 6/01/96 | 61.47 | 60.03 | 56.66 |
| | 3/30/98 | 68.59 | 66.93 | 60.06 |
| | 4/26/98 | 67.44 | 66.96 | 62.23 |
| | 5/27/98 | 67.33 | 66.63 | 65.01 |
| | 6/04/98 | 70.75 | 69.45 | 69.35 |
| | 6/10/98 | 68.43 | 68.30 | 65.64 |
| MCO | 4/28/97 | 59.57 | 57.31 | 55.73 |
| | 5/27/97 | 68.48 | 66.31 | 65.52 |
| | 10/27/97 | 53.27 | 51.63 | 49.40 |
| | 2/23/98 | 71.12 | 69.59 | 65.05 |
| BOS | 5/31/98 | 51.37 | 50.63 | 44.03 |
| | 7/23/98 | 58.66 | 55.57 | 56.86 |
| MEM | 6/09/94 | 59.80 | 57.76 | 52.45 |
| | Average | 63.56 | 62.08 | 59.07 |

To optimize the large-scale filter, 43 different filters were run with filter aspect ratios ranging from 1:1 through 9:1 (see Appendix A). The areas of the filters ranged from 200 $km^2$ to over 7000 $km^2$. Each case was run with the range of filters, and the case was completely scored using the scoring techniques previously described.

In Figure 2, the standard deviation in CSI among all the different filters is shown for each line storm case. It is clear that certain cases, such as the 30 March 1998 narrow line storm in DFW (Figure 3), are more sensitive to filter sizes and shapes than others.

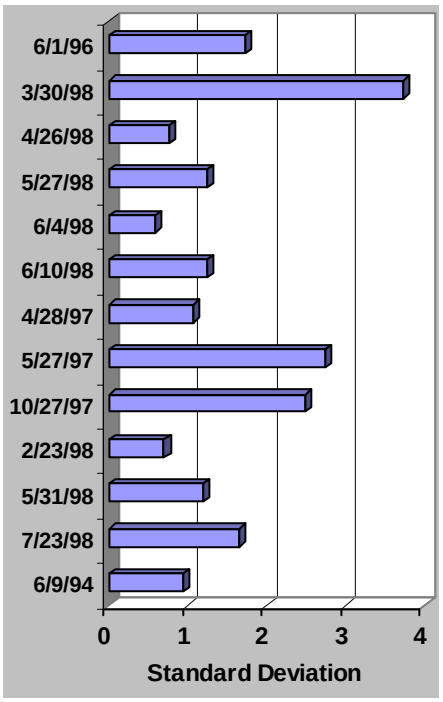


*Figure 2. Standard deviation of CSI scores over the different filters for each line storm.*

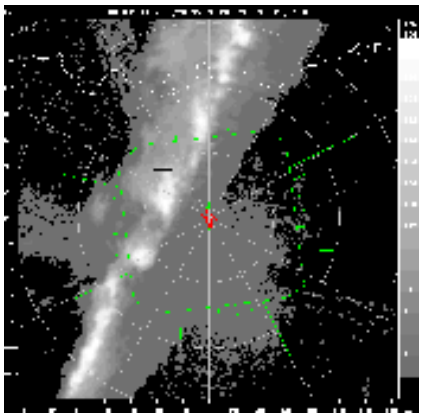

*Figure 3. VIL for March 30, 1998, in Dallas, TX, at 22:57.*

Figure 4 presents the average CSI over all 13 cases as a function of filter size. Separate curves for five of the aspect ratios considered are shown. The legend for this figure is in units of km$^2$, but all filter sizes from here forward will refer to pixels, where each pixel is 4 km x 4 km. The best average rectangular filter was 3x17 (6:1), and the best square filter was 7x7. The 3x17 rectangular filter is virtually identical to the 5x21 elliptical filter used by the TCWF in 1998 (the only difference being a few "wing" pixels), and the average CSI values compare closely.

Determining the "best" filter overall requires compromise, since each case day has a different optimal filter. The optimal filter size (both rectangular and square) for each case is illustrated in Figure 5. This graphs shows the difference in CSI between the optimal rectangle (or square) and the unfiltered CSI. Filtering prior to tracking improves forecast accuracy in every case. There are two days where optimal square filters outperform the rectangular filters. However, on days like March 30, 1998, rectangular filtering improves accuracy substantially. For challenging case days like May 31, 1998 in Boston, MA, filtering the image results in a proportionally large increase in forecast accuracy. (Absolute CSI values are given in Table 1.)

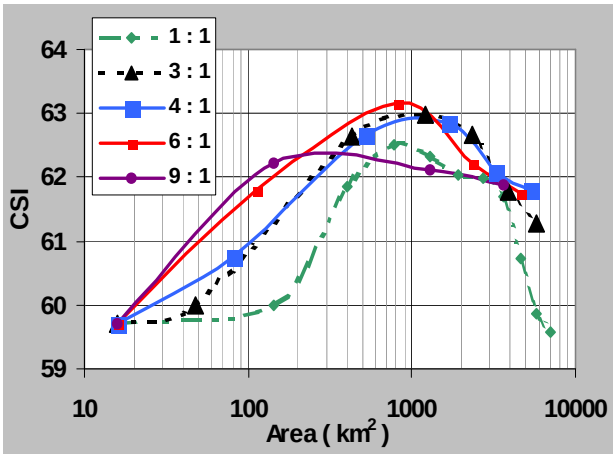


*Figure 4. Average CSI values for 13 line storm cases for five different filter aspect ratios: 1:1, 3:1, 4:1, 6:1, and 9:1, where an area equal to 16 describes the case where no filtering of the image is done.*

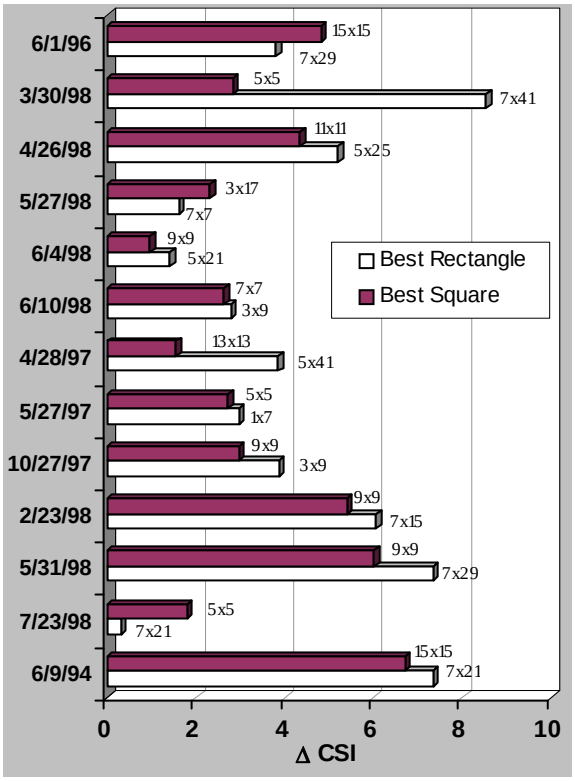


*Figure 5. Difference in CSI between the optimal rectangular filter (light bars) or square filter (dark bars) and no filter for each case. The dimensions of the optimal filter, in pixels, are annotated on the graph.*

Without selecting a matched, optimal filter in real time, the "average" optimal filter would have to be used. Figure 6 illustrates the differences in CSI between the best average rectangular filter (3x17) or the best average square filter (7x7) and the unfiltered CSI for each case. On four case days, using either the 3x17 or 7x7 filter causes a lowering of the CSI below the unfiltered score. However, on other days, there is a significant improvement by using a rectangular filter.

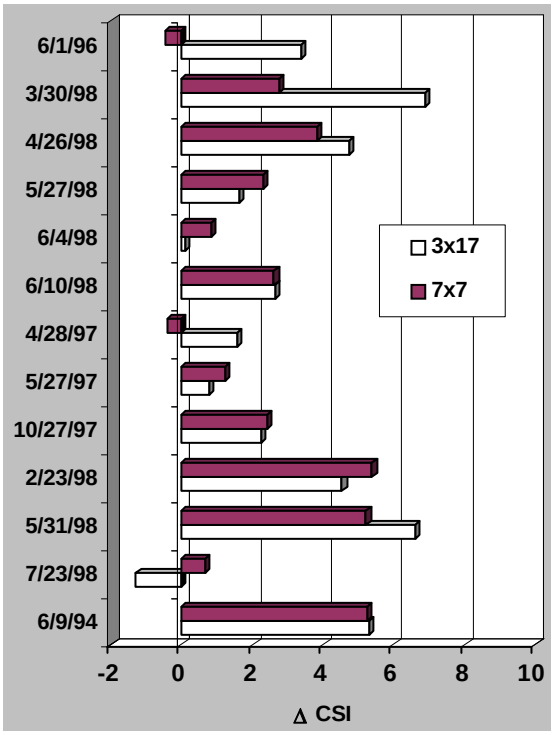


*Figure 6. Difference in CSI between the best average rectangular filter (3x17 – light bars) or square filter (7x7 – dark bars) and no filter for each case. Negative values indicate that the unfiltered CSI was higher than the filtered CSI.*

## 4. Summary

The Terminal Convective Weather Forecast product provides a solution for a user community that currently has very limited or no short-term convective forecast information. To improve the level of skill of the TCWF, we evaluated the size and the shape of the scale-selecting filter used prior to correlation tracking. This filtering is an integral component of the Growth and Decay Tracker. We found that the best average filter was a 3x17 rectangular filter. This result may be related to the fact that the tracker parameters were optimized using the nearly identical 5x21 elliptical filter. The choice of tracker parameters alone can greatly influence the resultant performance.

This study has used filtering as a preprocessing step to correlation tracking, to extract a scale for which pattern motion (over a 12-min interval) can be detected. Waiting 12 min between successive images to be correlated has already mitigated some of the benefits of filtering. Larger changes in CSI between filtered and unfiltered runs are observed for shorter time intervals, but so are lower absolute CSI values. Also, in every case, the *unfiltered* image was advected to produce the forecast. Studies by Zawadzki (1973) and others indicate results could be further improved by applying some smoothing to the image prior to or after advecting, although this will be less pronounced for data at 4 km resolution than at 1 km.

Future efforts will include filter optimization for 30, 90 and 120 min forecasts. The filters must also be applied to other types of convection including air mass storms to verify that the optimal line storm settings do not lower the overall forecast skill. Our goal is to continually improve the TCWF so that in the upcoming years it may be considered for operational implementation within ITWS and WARP (Weather and Radar Processor) preplanned product improvement programs, and perhaps in the NEXRAD system.

## 5. References


Bellon, A. and I. Zawadzki, 1994: Forecasting of hourly accumulations of precipitation by optimal extrapolation of radar maps. *Journal of Hydrology*, **157**, 211-233.

Forman, B.E., *et al.,* 1999: Aviation User Needs for Convective Weather Forecasts. 8th Conf. on Aviation Meteorology.

Hallowell, *et al*., 1999: The Terminal Convective Weather Forecast Demonstration at the DFW International Airport, 8th Conf. on Aviation Meteorology.

Wilson, J.W., 1966: Movement and predictability of radar echoes. NSSL Tech Memo, No. 28, Norman, OK. 30 pp.

Wolfson, *et al*., 1999: The Growth and Decay Storm Tracker, 8th Conf. on Aviation Meteorology.

Zawadzki, I.I., 1973: Errors and fluctuations of raingauge estimates of areal rainfall. *J. Hydrol*., **18**: 243-255.


## Appendix A.

Below is a summary of all filter sizes tested in this study. Filter dimensions are given in pixels.

| Aspect Ratio | Filter Sizes |
|---|---|
| 1:1 | No filter; 3x3, 5x5, 7x7, 9x9, 11x11,13x13, 15x15, 17x17, 19x19, 21x21 |
| 2:1 | 3x5, 3x7, 5x11, 7x15, 9x19, 13x25, 15x31 |
| 3:1 | 1x3, 3x9, 5x15, 7x21, 9x27, 11x33 |
| 4:1 | 3x11, 5x21, 7x29, 9x37 |
| 5:1 | 1x5, 3x15, 5x25, 7x35, 9x45 |
| 6:1 | 3x17, 5x29, 7x41 |
| 7:1 | 1x7, 3x21, 5x35 |
| 8:1 | 3x23, 5x41 |
| 9:1 | 1x9, 3x27, 5x45 |